Hydrogen Activation by Frustrated and Not So Frustrated Lewis Pairs Based on Pyramidal Lewis Acid 9-Boratriptycene: A Computational Study

Anna V. Pomogaeva and Alexey Y. Timoshkin*

Read Online

| ACCESS | Metrics & More | Article Recommendations | SI Supporting Information |

ABSTRACT: Structural features and reactivity of frustrated Lewis pairs (FLPs) formed by pyramidal group 13 Lewis acids based on 9-bora and 9-alatriptycene and bulky phosphines P^tBu_3, PPh_3, and PCy_3 are considered at the M06-2X/def2-TZVP level of theory. Classic FLP is formed only in the $B(C_6Me_4)_3CH/P^tBu_3$ system, while both FLP and donor−acceptor (DA) complex are observed in the $B(C_6F_4)_3CF/P^tBu_3$ system. Formation of DA complexes was observed in other systems; the $B(C_6H_4)_3CH·P^tBu_3$ complex features an elongated DA bond and can be considered a "latent" FLP. Transition states and reaction pathways for molecular hydrogen activation have been obtained. Processes of heterolytic hydrogen splitting are energetically more favored in solution compared to the gas phase, while activation energies in the gas phase and in solution are close. The alternative processes of hydrogenation of B−C or Al−C bonds in the source pyramidal Lewis acids in the absence of a Lewis base are exergonic but have larger activation energies than those for heterolytic hydrogen splitting. The tuning of Lewis acidity of 9-boratriptycene by changing the substituents allows one to control its reactivity with respect to hydrogen activation. Interestingly, the most promising system from the practical point of view is the DA complex $B(C_6H_4)_3CH·P^tBu_3$, which is predicted to provide both low activation energy and thermodynamic reversibility of the heterolytic hydrogen splitting process. It appears that such "not so frustrated" or "latent" FLPs are the best candidates for reversible heterolytic hydrogen splitting.
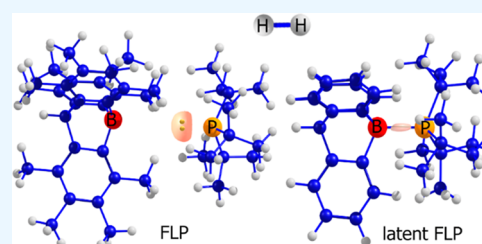
INTRODUCTION

After the discovery of frustrated Lewis pairs (FLPs) by Stephan et al. in 2006,[1] Lewis acid−base group 13−15 compounds emerged as powerful alternatives to the transition metals in catalysis.[2,3] Catalytic activity toward several processes has been demonstrated.[4−7] The use of 13−15 group element catalysts completely excludes contamination by traces of hazardous transition metals. Despite the long history of molecular H_2 activation by FLP, this chemistry remains the prospective field of research, as demonstrated in the recent perspective article by Stephan.[8] Due to the high potential for practical applications, search for novel catalytic systems for hydrogen activation based on group 13−15 element compounds with tunable properties continues.[9]

Lewis acidity is an important factor for the creation of the catalytic system since weak Lewis acids will not be catalytically active. On the other hand, very strong Lewis acids will form very stable reaction products, which will prevent the creation of the catalytic cycle. Therefore, development of group 13 Lewis acids with tunable Lewis acidity is an important task and is a focus of ongoing research.[10−13] In most of the works, the tuning of Lewis acidity is achieved by varying the substituents on the group 13 center by introduction of perfluorinated moieties, which strongly increases the Lewis acidity.[14]

Since upon complex formation, group 13 Lewis acids undergo structural reorganization from the planar geometry in the free

Lewis acid to the pyramidal in the complex, the energy required for this reorganization makes the interaction energy less exothermic. Therefore, another way to increase the Lewis acidity is to create compounds with an already pyramidalized group 13 Lewis center.[15] The high potential of group 13 pyramidal Lewis acids was pointed out based on the results of quantum-chemical computations.[16−18]

Experimental and computational studies of the chemistry of nonplanar group 13 Lewis acids were reviewed in 2020 by Berionni et al.[19] Early examples of the pyramidal Lewis acids include borabarrelene and benzaborabarrelene, which were isolated as pyridine complexes by Piers.[20] The classical example of pyramidal group 13 Lewis acid is boraadamantane,[21] which forms with azaadamantane a very strongly bound molecular complex, stable in air.[22] Systems based on bora- and ala-adamantane scaffolds connected by rigid aromatic spacers were designed and computationally studied.[23] Results indicate the principal possibility of hydrogen activation by group 13−15

Scheme 1. Experimentally Known 9-Boratriptycene Derivatives, Isolated as Complexes with Lewis Bases[a]
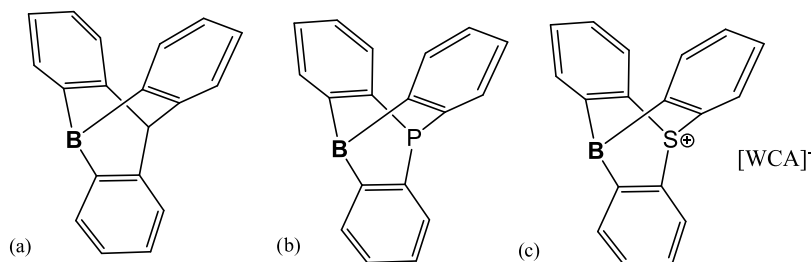
[a] (a) $B(C_6H_4)_3CH$,[26] (b) $B(C_6H_4)_3P$,[25] (c) $B(C_6H_4)S^+$.[28]

adamantane-based FLPs, with donor and acceptor fragments separated by a rigid spacer.[23]

Another family of pyramidalized group 13 Lewis acids is based on 9-boratriptycene (Scheme 1a). Since 9-boratriptycene, 9-alartriptycene, and their perfluorinated derivatives were computationally confirmed as strong pyramidal Lewis acids,[17] computational studies of their reactivity followed. Gilbert[18] predicted that perfluorinated 9-boratriptycene forms a stable complex with P^tBu_3, which is predicted to exothermically activate nitrous oxide. It was computationally demonstrated that donor−acceptor (DA) cryptands, featuring pyramidal spatially separated Al and N atoms, are able to exothermically form complexes with noble gases argon and krypton[16] and activate molecular hydrogen.[24] Fluorination of 9-boratriptycene significantly increases its Lewis acidity,[17] making $B(C_6F_4)_3CF$ a Lewis superacid.[15]

The experimental chemistry of 9-boratriptycene derivatives started in 2019 when Berionni reported a B−P derivative (Scheme 1b).[25] One year later, the parent 9-boratriptycene $B(C_6H_4)_3CH$ (Scheme 1a) was obtained in a CD_2Cl_2 solution in equilibrium with an $[R_4P]^+$ $[B(C_6H_4)_3CH\{NTf_2\}]^-$ ion pair and isolated in the form of molecular complexes with Et_2O, Py, PPh_3, 9-phosphatriptycene, and P^tBuPh_2.[26] The B−P bond distance in $B(C_6H_4)_3CH·PPh_3$ (1.976(4) Å[26]) is the shortest among known complexes with phosphines bearing aromatic substituents. More recently, cationic pyramidal LA based on the pyrazabole-bridged ansa-ferrocene was reported by Henkelmann et al. in 2022.[27] Sulfur-containing cationic derivatives of 9-boratriptycene (Scheme 1c) were experimentally realized by the Berionni group.[28] Formal replacement of the CH group in the aromatic ring of $B(C_6H_4)_3CH$ by the nitrogen atom results in 1-aza-9-boratriptycene, which may be considered an intramolecular FLP. Its reactivity toward C−H activation was computationally explored.[29]

The data on Lewis acidity of 9-boratriptycene vary depending on the used LA scale. The Gutmann acceptor number[30] of 9-boratriptycene (76[26]) is slightly smaller than that of $B(C_6F_5)_3$ (76−82[31]), indicating that 9-boratriptycene is a weaker LA than $B(C_6F_5)_3$ with respect to triethylphosphineoxide. In contrast, IR spectroscopy data show that the C≡N shift in $B(C_6H_4)_3CH·CH_3CN$ and the C=O shift in $B(C_6H_4)_3CH·EtOAc$ adducts are larger than that in the corresponding complexes of $B(C_6F_5)_3$. This indicates that 9-boratriptycene is a stronger LA than $B(C_6F_5)_3$.[26] Computed dissociation enthalpies of complexes with ammonia indicate that 9-boratriptycene is a much stronger Lewis acid than $B(C_6F_5)_3$.[17]

One of the avenues of the FLP design is to prevent the direct formation of the complex between components. This can be achieved using bulky organic substituents on the phosphine. Thus, tris *tert*-butyl phosphine P^tBu_3 is widely used as an FLP

component. The FLP based on $B(C_6F_5)_3$ and P^tBu_3 was extensively studied both experimentally and computationally.[32−34] Another practical approach to avoid or hinder the direct DA bond formation is to carry out the reaction of molecular hydrogen with mixtures of solid LA and LB.[35] In such a case, the process of hydrogen activation supposedly occurs in the area of the contact between solid LA and LB particles, but completing the reaction requires a prolonged (up to 10 days) time.[35]

Although the mechanism of hydrogen activation by both intra- and intermolecular FLP based on $B(C_6F_5)_3$ is well described,[32−34,36,37] the FLPs based on pyramidal group 13 Lewis acids are much less studied. Herein, we computationally explore the potential of 9-boratriptycene and 9-alatriptycene and their derivatives (Scheme 2) to form FLPs with bulky

Scheme 2. Pyramidal Group 13 Lewis Acids, Considered in the Present Work[a]
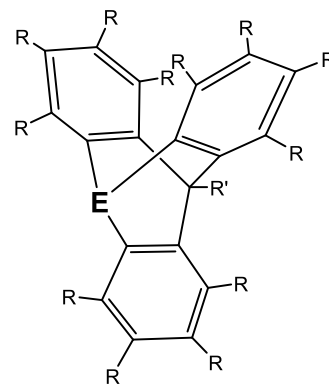
[a] E = B, R = H, F, Me; E = Al, R = H, F. R′ = F for R = F, and R′ = H for R = H, Me.

phosphines and their activity toward molecular hydrogen activation. In particular, we are interested in the influence of the central atom (B/Al), the substituents on Lewis acid (H, F, Me) and Lewis base (^tBu, Ph, Cy) on the stability of the DA complexes, the energetics of FLP formation, and their reactivity toward molecular hydrogen. The alternative hydrogenation of B−C and Al−C bonds in the absence of the Lewis base is also reported.

■ COMPUTATIONAL DETAILS

All computations were performed at the M06-2X/def2-TZVP[38,39] level of theory using the Gaussian 16 program package.[40] Vibrational frequency analysis was performed to define the transition states (TS) and local minima at the potential energy surface (PES). The intrinsic reaction
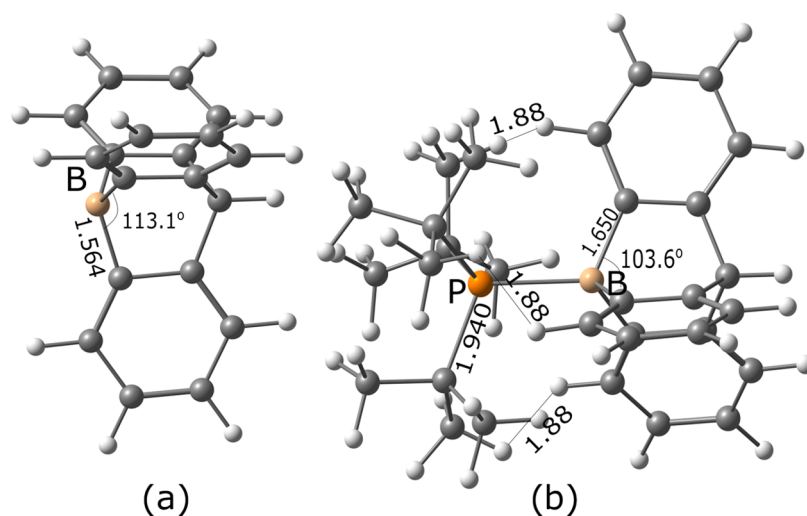
Figure 1. Optimized geometries of 9-boratriptycene (a) and its DA complex with P^tBu_3 (b).
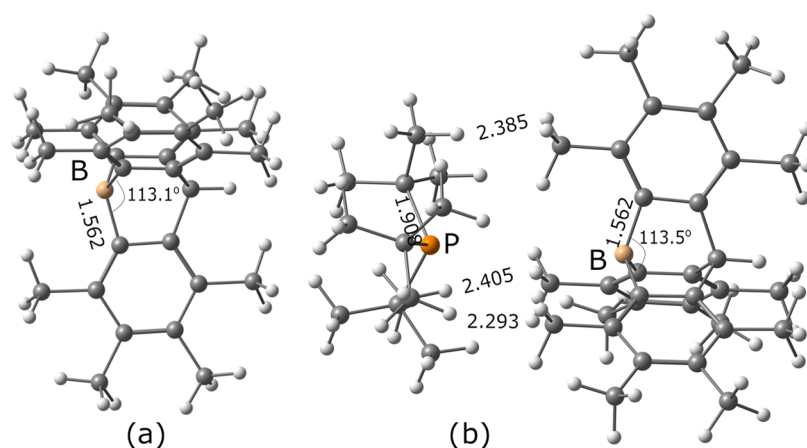

Figure 2. Optimized geometries of $B(C_6Me_4)_3CH$ (a) and its FLP with P^tBu_3 (b).

Table 1. Selected Structural (E−P Interatomic Distance R_{DA} in Å, Increase in the Pyramidalization Degree of LA $\Delta\alpha$ in Degrees) and Energetic Characteristics of Studied Systems: Reorganization Energies E_r of Lewis Acid and Lewis Base, Energy of the DA Bond E_{DA}, and Standard Enthalpies $\Delta_{diss}H°_{298}$ and Gibbs Energies $\Delta_{diss}G°_{298}$ of Dissociation Into Components (All in kJ·mol^{-1}) and the Energy Difference between the LUMO of Free LA and the HOMO of Free LB, E_{HL} (in eV)[a]

compound	R_{DA}	$\Delta\alpha$	$E_r(LA)$	$E_r(LB)$	E_{DA}	$\Delta_{diss}H°_{298}$	$\Delta_{diss}G°_{298}$	E_{HL}
$B(C_6Me_4)_3CH\cdots P^tBu_3$	4.944	0.4	1.1	0.3	27	19	−27.7	6.57
$B(C_6H_4)_3CH\cdot P^tBu_3$	2.176	28.5	86.9	64.1	225	56	−5.6	6.22
$B(C_6H_4)_3CH\cdot PCy_3$	1.988	26.4	68.2	22.6	299	196	128.5	6.16
$B(C_6H_4)_3CH\cdot PPh_3$	1.962	24.2	58.1	13.6	269	188	125.5	6.48
$B(C_6F_4)_3CF\cdot P^tBu_3$	2.152	31.7	116.8	156.9	306	41	−27.0	4.64
$B(C_6F_4)_3CF\cdots P^tBu_3$	3.807	5.7	5.4	2.9	41	25	−25.2	4.64
$B(C_6F_4)_3CF\cdot PCy_3$	2.014	28.9	86.8	37.0	390	251	182	4.58
$B(C_6F_4)_3CF\cdot PPh_3$	1.983	26.2	73.8	23.9	335	229	154.6	4.90
$Al(C_6H_4)_3CH\cdot P^tBu_3$	2.507	21.2	26.9	8.3	219	174	114.8	5.56
$Al(C_6H_4)_3CH\cdot PPh_3$	2.422	16.7	15.0	16.6	192	154	105.1	5.82
$Al(C_6F_4)_3CF\cdot P^tBu_3$	2.619	24.4	50.9	12.3	264	189	129.2	3.93
$Al(C_6F_4)_3CF\cdot PPh_3$	2.404	18.6	18.8	17.9	265	222	170.6	4.19

[a]M06-2X/def2-TZVP level of theory.

coordinate (IRC) method[41] followed by full geometry optimization was used to determine the reaction products connected by a given TS. The local quadratic approximation method[42] with step size along the reaction path of 0.2 Bohr was used in the case of systems with a very flat PES. Estimation of the

influence of the solvent was performed by single-point energy computations at optimized gas-phase geometries of the compounds and TS using the SMD model.[43] Reorganization energies E_r of LA and LB are obtained as the difference of the total energies of the LA or LB fragment in the geometry of the
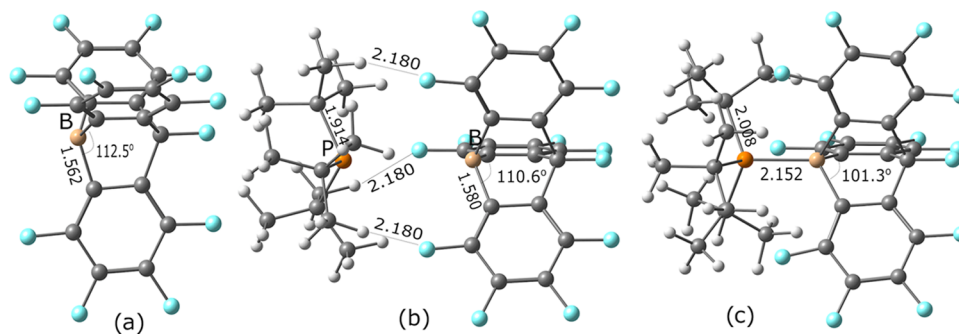
Figure 3. Optimized geometries of $B(C_6F_4)_3CF$ (a), its FLP with P^tBu_3 (b), and its DA complex with P^tBu_3 (c).

DA complex and in the gas-phase optimized geometry of LA or LB. The energy of the DA bond, E_{DA}, was computed as $E_{DA} = E_{diss} + E_r(LA) + E_r(LB)$, where E_{diss} is the energy of dissociation of the DA complex into components.

RESULTS AND DISCUSSION

Structures and Stability of 9-Boratriptycene Derivatives and Their DA Complexes with Phosphines. First, let us consider the structural features of the individual pyramidal Lewis acids. The triptycene scaffold enforces pyramidalization of the group 13 Lewis center. The pyramidalization degree can be quantitatively characterized by the parameter α, defined as $360°$ minus a sum of valence C−E−C angles (E = B, Al). The value of $\alpha = 0$ corresponds to the planar arrangement, while $\alpha = 31.5$ indicates ideal tetrahedral coordination. For the parent $B(C_6H_4)_3CH$ (Figure 1a), $\alpha = 20.6°$, which indicates a significant degree of pyramidalization. Methyl substituents slightly reduce the pyramidalization ($\alpha = 19.7°$), while fluorination makes $B(C_6F_4)_3CF$ (Figure 2a) slightly more pyramidal ($\alpha = 22.4°$). Replacement of the central boron atom by aluminum leads to a noticeable increase in the pyramidalization degree ($\alpha = 37.9$ and $46.8°$ for the hydrogenated and fluorinated derivatives, respectively), which significantly exceeds the value of α for the ideal tetrahedral geometry. This is a result of pure geometry factors: combination of a rigid triptycene core and longer Al−C distance forces the aluminum atom to be more pyramidal. Computational studies indicate that the LUMO is an almost pure (more than 99%) p-orbital for both B and Al derivatives. Aluminum−nitrogen DA cryptands constructed on the basis of Al-containing pyramidalized LA based on the triptycene framework are predicted to be highly reactive toward noble gases[16] and molecular hydrogen activation.[24]

Now, we turn our attention to the structural and energetic characteristics of the interaction products of pyramidal LA (Scheme 2) with P^tBu_3, PCy_3, and PPh_3. Selected characteristics of the formed DA complexes and FLP are provided in Table 1. For the complexes of group 13 metal halides with ammonia, a correlation between the pyramidalization degree and the DA bond distance was observed.[44] Therefore, the increase of the pyramidalization degree (value of $\Delta\alpha$ − the difference of α in the complex and in the free LA) can be used as an indicator of DA bond formation.

Among the considered systems, only in the case of the $B(C_6Me_4)_3CH\cdots P^tBu_3$ system (Figure 2b) geometry optimization in the gas phase converges to a structure without a direct DA bond between boron and phosphorus atoms. The methyl substituents on 9-boratriptycene provide additional steric strain and decrease the acceptor ability of LA, leading to the B⋯P

interatomic distance of 4.94 Å, which is significantly larger than the sum of the van der Waals radii of boron and phosphorus atoms (3.72 Å).[45] Both LA and LB are almost unperturbed (reorganization energies are only 0.3 and 1.1 kJ mol^{-1}), $\Delta\alpha = 0.4$, and the standard dissociation enthalpy of $B(C_6Me_4)_3CH\cdots P^tBu_3$ into components is only 19 kJ mol^{-1}.

An interesting situation was observed in the $B(C_6F_4)_3CF−P^tBu_3$ system. In addition to the DA complex $B(C_6F_4)_3CF\cdot P^tBu_3$ (Figure 3c) reported earlier by Gilbert,[18] the second, FLP-type minimum $B(C_6F_4)_3CF\cdots P^tBu_3$ was obtained (Figure 3b) with a B⋯P interatomic distance of 3.807 Å, which also slightly exceeds the sum of van der Waals radii of B and P. A relaxed potential energy scan along the B−P distance showed at 2.8 Å an energy barrier of ca. 56 kJ·mol^{-1} relative to the energy of the DA complex (Figure S1). The FLP-type structure $B(C_6F_4)_3CF\cdots P^tBu_3$ is only 26 kJ mol^{-1} higher in energy than the DA complex $B(C_6F_4)_3CF\cdot P^tBu_3$ and may be stabilized by interatomic contacts F⋯H of 2.18 Å. Similar stabilization via interaction between H atoms of phenyl and F atoms of C_6F_5 groups was recently noted for the $B(C_6F_5)_3\cdot EPh_3$ complexes (E = As, Sb) by Ketkov et al.[46] Dissociation enthalpy of 25 kJ mol^{-1} and reorganization energies of the fragments (2.9 and 5.4 kJ mol^{-1}) for $B(C_6F_4)_3CF\cdots P^tBu_3$ are slightly larger compared to those for $B(C_6Me_4)_3CH\cdots P^tBu_3$. The entropy factor dissociation of these two weakly bound systems into components at 298 K is exergonic by 25−28 kJ mol^{-1}. Dissociation of the DA complex $B(C_6F_4)_3CF\cdot P^tBu_3$ into components at 298 K is also exergonic by 27 kJ mol^{-1} (Table 1). In this complex, the B−P bond distance of 2.152 Å is elongated compared to complexes of $B(C_6F_4)_3CF$ with PCy_3 and PPh_3, which are considered to be weaker σ-donors than P^tBu_3.[47,48] This DA bond elongation is a result of a steric repulsion, which manifests itself in elongation of P−C bond lengths by 0.098 Å compared to free P^tBu_3 and a notably larger degree of pyramidalization of the boron atom $\Delta\alpha$ than in the FLP-type $B(C_6F_4)_3CF\cdots P^tBu_3$ isomer (Table 1).

In all other studied systems, geometry optimization results in complexes with the DA bond. Interestingly, the complex of the parent 9-boratriptycene with a bulky P^tBu_3 is different from the other DA complexes. $B(C_6H_4)_3CH\cdot P^tBu_3$ (Figure 1b) features a significantly elongated DA bond distance of 2.176 Å, which is 0.18−0.21 Å larger than in complexes with PCy_3 and PPh_3. The P−C bond distance in the P^tBu_3 fragment in the complex is elongated by 0.029 Å with respect to 1.910 Å in free P^tBu_3. This bond elongation is a result of the large steric repulsion between components, which manifests itself in large reorganization energies of $B(C_6H_4)_3CH$ and P^tBu_3 (87 and 64 kJ mol^{-1}, respectively). The Lewis acid becomes significantly more pyramidal ($\Delta\alpha = 28.5$). Despite the DA bond energy being large (225 kJ mol^{-1}), the gas-phase dissociation enthalpy of the
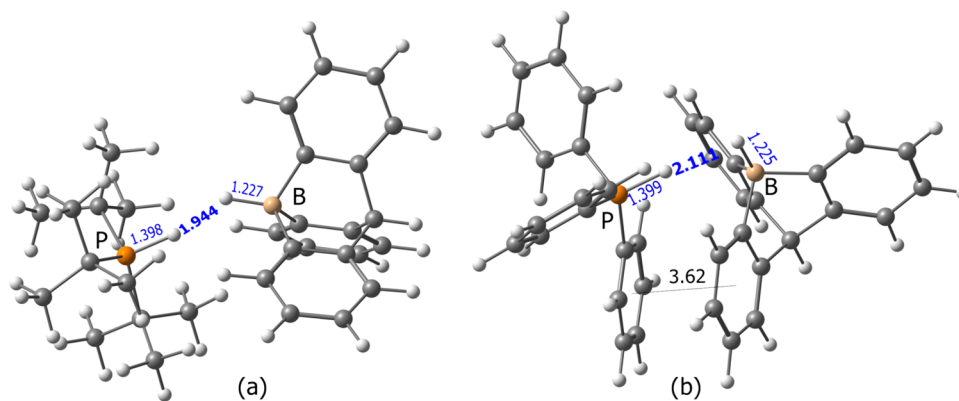
Figure 4. Optimized geometries of $[HP^tBu_3]^+\cdots[HB(C_6H_4)_3CH]^-$ (a) and $[HPPh_3]^+\cdots[HB(C_6H_4)_3CH]^-$ (b).

Table 2. Thermodynamic Characteristics of Heterolytic Hydrogen Splitting[a]

LA, LB	process (1)				process (2)			
	$\Delta_{(1)}E$	$\Delta_{(1)}H°_{298}$	$\Delta_{(1)}G°_{298}$	$\Delta_{(1)}S°_{298}$	$\Delta_{(2)}E$	$\Delta_{(2)}H°_{298}$	$\Delta_{(2)}G°_{298}$	$\Delta_{(2)}S°_{298}$
$B(C_6Me_4)_3CH, P^tBu_3$	−53.8	−29.8	55.3	−285.4	−28.5	−10.4	27.6	−127.6
$B(C_6H_4)_3CH, P^tBu_3$	−106.5	−84.3	−4.6	−267.3	−32.4	−28.1	−10.2	−59.9
$B(C_6H_4)_3CH, PCy_3$	−159.5	−135.8	−48.7	−292.1	48.4	60.0	79.8	−66.2
$B(C_6H_4)_3CH, PPh_3$	−108.9	−86.9	8.9	−321.3	88.4	101.2	131.4	−101.3
$B(C_6F_4)_3CF, P^tBu_3$	−243.0	−218.4	−139.4	−264.8	−184.5	−177.8	−167.2	−38.4
$B(C_6F_4)_3CF, PCy_3$	−286.4	−259.0	−163.1	−321.9	−20.4	−7.8	18.7	−88.8
$B(C_6F_4)_3CF, PPh_3$	−223.0	−199.3	−103.6	−321.1	14.7	29.5	51.0	−72.2
$Al(C_6H_4)_3CH, P^tBu_3$	−106.0	−89.4	−9.1	−269.2	77.5	84.2	105.7	−72.0
$Al(C_6H_4)_3CH, PPh_3$	−81.7	−66.1	26.1	−309.0	78.9	87.9	131.2	−145.1
$Al(C_6F_4)_3CF, P^tBu_3$	−203.6	−185.4	−103.1	−276.3	−3.2	3.5	26.1	−75.8
$Al(C_6F_4)_3CF, PPh_3$	−165.0	−148.2	−61.5	−290.8	63.3	73.3	109.1	−119.9

[a]Reaction energies ΔE, standard reaction enthalpies $\Delta H°_{298}$, Gibbs energies $\Delta G°_{298}$ (all in kJ·mol^{-1}), and standard reaction entropies $\Delta S°_{298}$ in J·mol^{-1}K^{-1} for processes (1) and (2) in the gas phase. M06-2X/def2-TZVP level of theory.

$B(C_6H_4)_3CH\cdot P^tBu_3$ complex into components is only 56 kJ mol^{-1}; dissociation of the complex is predicted to be slightly exergonic already at room temperature. Thus, $B(C_6H_4)_3CH\cdot P^tBu_3$ may be considered a "latent" FLP with potentially high reactivity.

The σ-donor ability of the considered phosphines decreases in the order $P^tBu_3 \geq PCy_3 > PPh_3$.[47,48] This order correlates with the trends in structural and energetic characteristics of their DA complexes. Thus, the degree of additional pyramidalization ($\Delta\alpha$) on the boron atom due to the interaction of $B(C_6H_4)_3CH$ with the Lewis base decreases according to this trend. Similarly, reorganization energies of both the phosphine and B-$(C_6H_4)_3CH$ fragments of the DA complex decrease in the same order. The dissociation energies, as well as the energies of the DA bond, are larger for complexes with PCy_3 compared to that with PPh_3 for both $B(C_6H_4)_3CH$ and $B(C_6F_4)_3CF$. The computed B−P distance in $B(C_6H_4)_3CH\cdot PPh_3$ of 1.962 Å is slightly shorter compared to the experimental value of 1.976(4) Å in the solid state.[26] This compound features one of the shortest B−P bonds reported to date for R_3BPR_3 complexes (R − aryl group).[26] For minimizing steric repulsions, the aryl rings of 9-boratriptycene and the phenyl groups of the phosphine adopt a staggered conformation with CPBC torsion angles of about 44 in both the experimental solid state[26] and optimized gas phase structures. Within the framework of an NBO analysis, the B−P bond in $B(C_6H_4)_3CH\cdot PPh_3$ is a single covalent bond defined as a 0.64 B{s(22.1%)p$^{3.52}$(77.7%)} + 0.77P{s(31.9%)-p$^{2.13}$(68.0%)} combination of natural atomic orbitals.

With respect to complexes with triphenylphosphine, the fluorination of LA leads to a significant increase in the dissociation energy of the DA complex and a sharp decrease in the energy difference between the LUMO of the acceptor and the HOMO of the donor, which facilitates covalent bonding. Note that the B−P bond in $B(C_6F_4)_3CF\cdot PPh_3$ is longer by 0.021 Å than in $B(C_6H_4)_3CH\cdot PPh_3$, and in $B(C_6F_4)_3CF\cdot PCy_3$, it is longer by 0.026 Å than in $B(C_6H_4)_3CH\cdot PCy_3$, despite the larger acidity of perfluorinated LA, which may be attributed to steric repulsion by introducing F substituents.

In contrast to 9-boratriptycene, its heavy homologue 9-alatriptycene forms strong DA complexes with all studied phosphines. In practice, Al-containing Lewis acids are stronger than their B-containing analogues.[14,49] This is due to the much larger reorganization energy from planar to pyramidal conformation upon complex formation of the boron atom compared to Al.[17] In the case of 9-boratriptycene, the boron atom is already pyramidalized. Therefore, the replacement of the boron atom by aluminum leads to a decrease of the dissociation enthalpy of DA complexes of 9-alatriptycene and its fluorinated derivatives with PPh_3 (Table 1). This can be explained by the larger integral overlap for the smaller B atom compared to Al despite the fact that the LUMO of the Al-containing LA is lower by 0.66−0.71 eV than for the B-containing LA.

Thermodynamics of Heterolytic Hydrogen Splitting. Heterolytic H_2 splitting is a proton transfer to LB and hydride transfer to LA, resulting in ion pairs (Figure 4). A long dihydrogen bond is present in $[HP^tBu_3]^+\cdots[HB(C_6H_4)_3CH]^-$ (Figure 4a). In $[HPPh_3]^+\cdots[HB(C_6H_4)_3CH]^-$, the fragments

are arranged in a specific way to achieve favorable π-interaction between phenyl groups of the Lewis base and C_6H_4 rings of the Lewis acid (Figure 4b).

Thermodynamic characteristics of heterolytic H_2 splitting are summarized in Table 2.

Two processes were considered: formation of the contact ion pairs from the isolated LA, LB, and H_2 (process 1) and from the DA complex or FLP and H_2 (process 2).

$$LA + LB + H_2 = [HLB]^+ \cdots [HLA]^- \qquad (1)$$

$$LA \cdot LB + H_2 = [HLB]^+ \cdots [HLA]^- \qquad (2)$$
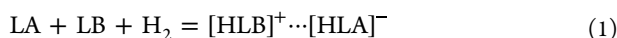
Reaction energies for process (1) are exothermic for all studied systems; in the case of fluorinated LA, the process is more exothermic by $112-134$ kJ mol^{-1} compared to hydrogen-substituted derivatives. Process (1) is the most exothermic for PCy_3 and more exothermic for P^tBu_3 than for PPh_3 for all studied Lewis acids except for $B(C_6H_4)_3CH$, where the reaction enthalpies are close for its complexes with P^tBu_3 and PPh_3. The entropy factor disfavors heterolytic hydrogen splitting, so reactions of the formation of ion pairs $[HP^tBu_3]^+ \cdots [HB-(C_6Me_4)_3CH]^-$, $[HPPh_3]^+ \cdots [HB(C_6H_4)_3CH]^-$, $[HPPh_3]^+ \cdots [HAl(C_6H_4)_3CH]^-$ from the components are endergonic.

Process (2) considers the reaction of molecular H_2 with the initially formed DA complexes. In this case, the reaction energy is exothermic only for the true FLP with P^tBu_3 and the "latent" FLP $B(C_6H_4)_3CH \cdot P^tBu_3$. Reactions (2) in the cases of the complexes of $B(C_6R_4)_3CR'$ with P^tBu_3 are exothermic by 28, 178, and 10 kJ·mol^{-1} for the parent, fluorinated, and methyl-substituted LA, respectively. In the case of the $Al(C_6F_4)_3CF \cdot P^tBu_3$ complex, the process of hydrogen splitting is almost athermal (3.5 kJ mol^{-1}). The standard Gibbs energy of process (2) is negative only for the reactions of molecular hydrogen with $B(C_6H_4)_3CH \cdot P^tBu_3$ and $B(C_6F_4)_3CF \cdot P^tBu_3$, which are thermodynamically favorable systems for heterolytic hydrogen splitting.

For the creation of catalytic systems, the reversible process, in which ΔG°_{298} is close to zero, is optimal.[50] Highly exergonic processes result in very stable reaction products, which will not participate in subsequent catalytic reactions. Therefore, based on the computed ΔG°_{298} values, the systems $B(C_6Me_4)_3CH \cdots P^tBu_3$, $B(C_6H_4)_3CH \cdot P^tBu_3$, and $Al(C_6F_4)_3CF \cdot P^tBu_3$ for which process (2) is either slightly exergonic (-5 kJ mol^{-1}) or slightly endergonic (55, 26 kJ mol^{-1}) appear to be potential candidates for the creation of catalytic systems. However, the energy barriers for hydrogen splitting are also very important factors. Therefore, in the next section, the reaction pathways will be presented and discussed.

Reaction Pathways for Molecular Hydrogen Activation. Reaction pathways for the boron-containing LA are presented in Figure 5. Heterolytic hydrogen splitting is a two-step process for the majority of $B(C_6R_4)_3CR'/LB$ pairs, similar to the case of hydrogen activation by $B(C_6F_5)_3/P^tBu_3$.[32–34] Optimized structures of selected TS and intermediates are provided in Figure 6. The first step is the capture of a hydrogen molecule by a Lewis acid with the formation of an intermediate (Figure 6b,f,i); the second step is heterolytic H_2 splitting with proton transfer to the Lewis base via TS2 (Figure 6c,g,j).

The transition state TS1 for the first step (Figure 6e) was located only for $B(C_6H_4)_3CH/P^tBu_3$ and $B(C_6H_4)_3CH/PCy_3$ pairs, and it is the highest point on PES (Figure 5) for these systems. It is a three-molecule $(LA \cdots LB \cdots H_2)$ transition state (Figure 6e), and the PES around this TS1 is extremely flat. The respective imaginary frequencies have values of only 23i and 21i
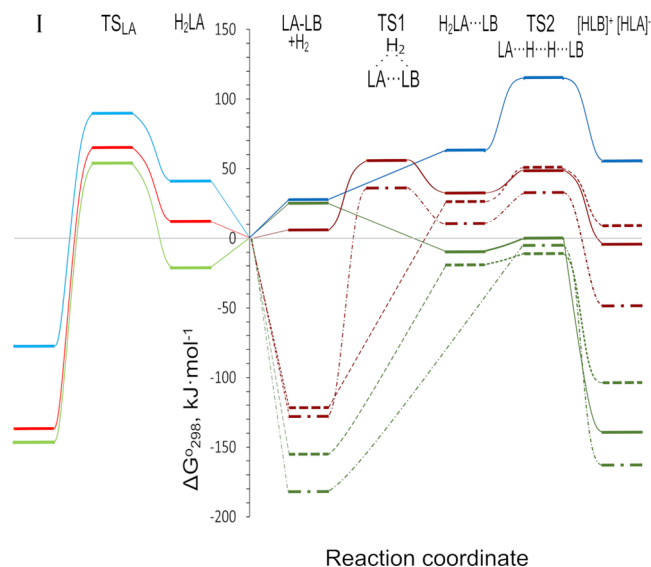

Figure 5. Reaction pathways for the hydrogenation of the B−C bond without LB (left side) and heterolytic H_2 splitting (right side) for the boron-containing LA. Color code: $B(C_6H_4)_3CH$ (red), $B(C_6Me_4)_3CH$ (blue), and $B(C_6F_4)_3CF$ (green); for the right side: Lewis bases: P^tBu_3 (lines), PPh_3 (dashed lines), and PCy_3 (dash-dot lines). The standard Gibbs energy values are given relative to the sum of the standard Gibbs energies of free components, $LA + LB + H_2$. M06-2X/def2-TZVP level of theory.

cm^{-1}. However, it should be noted that all three molecules $(LA \cdots LB \cdots H_2)$ are simultaneously involved in these low-frequency oscillations. The geometry optimization of the structures obtained by stepping forward and backward along the direction of the oscillation unambiguously resulted, on the one hand, in the formation of an $LA \cdot H_2 + LB$ intermediate (Figure 6f) and, on the other hand, in the formation of an $LA \cdot LB$ donor−acceptor complex (Figure 6d). Moreover, the IRC scan from the TS1 state for the $B(C_6H_4)_3CH/P^tBu_3$ system was obtained; subsequent optimization of the geometry of the resulting structures in the forward and backward directions resulted in a smooth descent to the DA complex and to the $B(C_6H_4)_3CH \cdot H_2 + P^tBu_3$ intermediate structure.

For the strongly bound DA complex $B(C_6H_4)_3CH \cdot PCy_3$, the first step of H_2 activation includes DA bond breaking and therefore the activation energy is high (155 kJ·mol^{-1}). In the case of the $B(C_6H_4)_3CH \cdot P^tBu_3$ complex, the dissociation energy is not large due to the pronounced steric repulsion between the components. Thus, the activation energy for the first step is only 45 kJ·mol^{-1}, which is similar to the one found for the $B(C_6F_5)_3/P^tBu_3$ pair (46 kJ·mol^{-1}).[34]

Thus, for the strongly bound DA complexes, the rate-limited step is the DA bond rupture (Figure 5). The energy barrier for the $B(C_6F_4)_3CF \cdot P^tBu_3$ to $B(C_6F_4)_3CF \cdots P^tBu_3$ transformation is ca. 56 kJ mol^{-1}, but the Gibbs energies of these structures at 298 K are almost equal. Starting from $B(C_6F_4)_3CF \cdots P^tBu_3$, the H_2 activation by this system is practically barrier-free (Figure 5) since both the $B(C_6F_4)_3CF \cdot H_2 + P^tBu_3$ intermediate and especially the resulting $[HP^tBu_3]^+ [HB(C_6F_4)_3CF]^-$ ion pair are lower in energy with respect to the FLP. The transition state for the first step was not located; the activation barrier for the second step is only 9 kJ mol^{-1} (Figure 5).

The methyl-substituted derivative, which does not form a DA bond with P^tBu_3, has a different energy profile. The first TS was not located, and the energetic stabilization of the H_2 molecule in
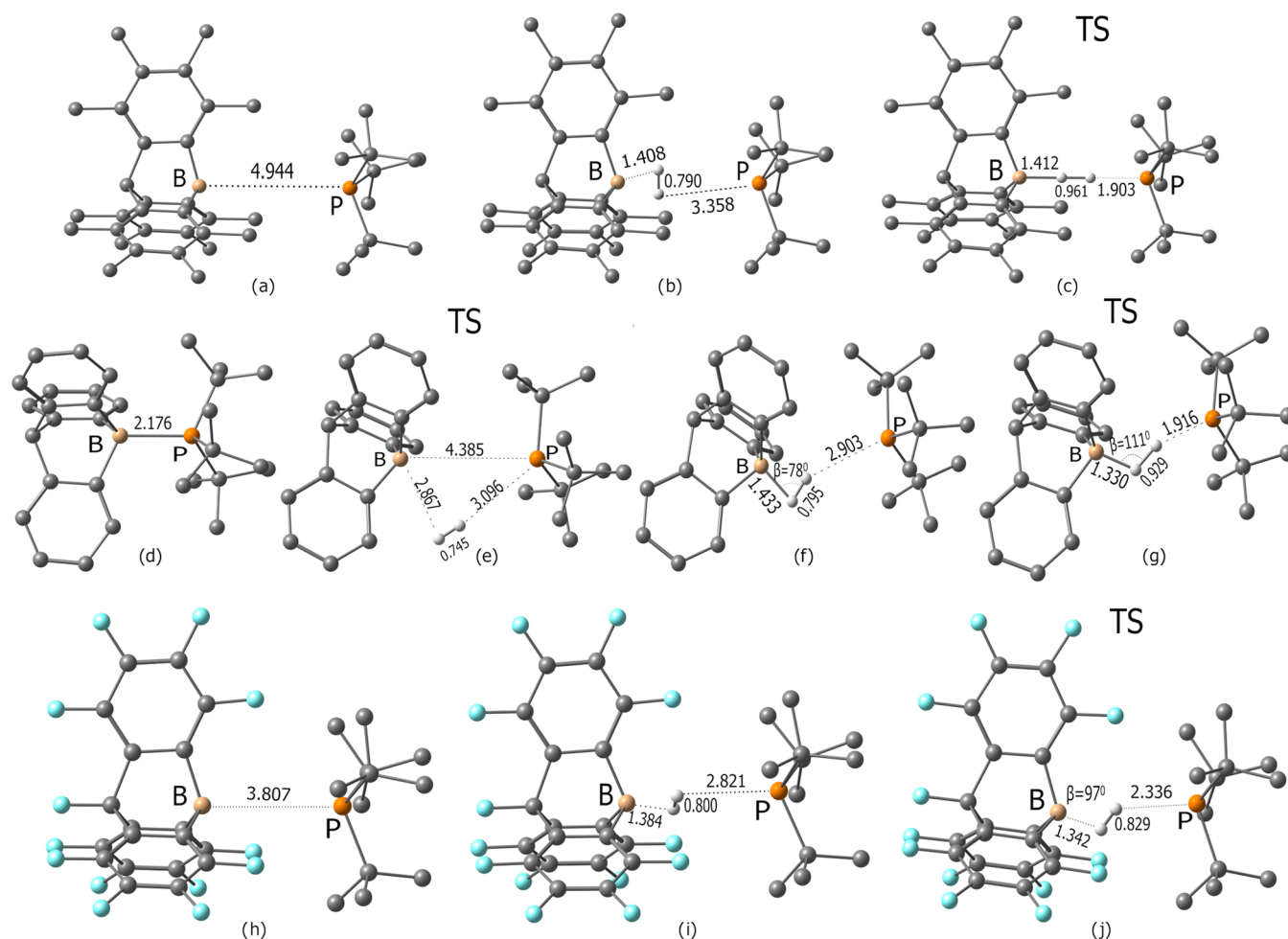
Figure 6. Optimized geometries for local minima and TS for molecular hydrogen activation. Hydrogen atoms bonded to carbon atoms are omitted for clarity. Top row: $B(C_6Me_4)_3CH/P^tBu_3$ system: (a) FLP, (b) $B(C_6Me_4)_3CH·H_2 + P^tBu_3$, (c) TS2; middle row: $B(C_6H_4)_3CH/P^tBu_3$ system, (d) DA complex, (e) TS1, (f) $B(C_6H_4)_3CH·H_2 + P^tBu_3$, (g) TS2; and bottom row: $B(C_6F_4)_3CF/P^tBu_3$ system, (h) FLP, (i) $B(C_6F_4)_3CF·H_2 + P^tBu_3$, (j) TS2. M06-2X/def2-TZVP level of theory.

Table 3. Gas-Phase Relative Energies ΔE and Relative Standard Gibbs Energies $\Delta G°_{298}$ (kJ·mol^{-1}) of the Intermediates and Transition States with Respect to the Sum of the Energies of Isolated Components LA + LB + H$_2$ [a]

system	ΔE	ΔE	$\Delta G°_{298}$	$\Delta G°_{298}$				
LA/LB	H$_2$LA···LB	TS	H$_2$LA···LB	TS	r(B−H)	r(H−H)	β	r(H−P)
$B(C_6Me_4)_3CH/P^tBu_3$	−36.4	12.7	62.8	114.7	1.412	0.961	180	1.903
$B(C_6H_4)_3CH/P^tBu_3$	−65.8	−46.4	32.2	48.3	1.330	0.929	110.8	1.916
$B(C_6H_4)_3CH/PCy_3$	−88.8	−64.8	10.5	32.4	1.324	0.936	99.8	1.925
$B(C_6H_4)_3CH/PPh_3$	−79.2	−53.6	25.9	49.0	1.311	0.992	96.1	1.813
$B(C_6F_4)_3CF/P^tBu_3$	−102.4	−98.3	−9.7	−0.2	1.342	0.829	97.2	2.336
$B(C_6F_4)_3CF/PCy_3$		−103.0		−5.2	1.400	0.797	73.4	2.891
$B(C_6F_4)_3CF/PPh_3$	−130.6	−123.6	−19.5	−10.5	1.328	0.900	89.9	2.045
$Al(C_6H_4)_3CH/P^tBu_3$	−180.1	−44.8	−86.1	44.1	1.744	0.963	107.4	1.829
$Al(C_6H_4)_3CH/PPh_3$	−165.3	−39.9	−89.4	54.2	1.721	1.045	99.5	1.718
$Al(C_6F_4)_3CF/P^tBu_3$	−91.4	−91.4	−1.3	0.8	1.876	0.792	89.0	2.551
$Al(C_6F_4)_3CF/PPh_3$		−110.5		−7.0	1.733	0.920	98.0	1.914

[a]Selected interatomic distances (in Å) and B−H−H angle β (deg) in TS2. The M06-2X/def2-TZVP level of theory.

the first intermediate is the smallest among considered systems (only 11 kJ mol^{-1}). The second, hydrogen splitting TS2, features almost a linear orientation of the H$_2$ molecule with respect to the B−P line (Figure 6c), resulting in the most pronounced polarization of the H$_2$ molecule. The importance of dihydrogen bonds for hydrogen splitting was noted by Repo et al.[51] The

difference in NPA charges between two H atoms in TS2 is 0.35e (NPA charges for H$^-$ and H$^+$ are −0.16 and +0.19e). A linear H−H−P orientation was observed for the intermediates and TS formed by DA cryptands based on boraadamantane[23] and indicates electron donation of the Lewis base to the antibonding σ^* orbital of the hydrogen molecule. The large difference in the

geometry of the first $B(C_6Me_4)_3CH$-H_2 + P^tBu_3 intermediate (Figure 6b) and TS2 (Figure 6c) contributes to the sizable (49 kJ·mol^{-1}) activation barrier between this intermediate and the final $[HP^tBu_3]^+[HB(C_6Me_4)_3CH]^-$ product. It should be noted that only for this system all intermediates and TS have Gibbs energies larger than the isolated LA, LB, and H_2.

Due to the larger Lewis acidity of H- and F-derivatives, the geometry of TS2 for all other studied systems (Figure 6g,j) is different from the one found for methyl-substituted 9-boratriptycene (Figure 6c). In these systems, the hydrogen molecule acts as a σ-donor of the electron density from the σ-bonding orbital to the LA, and therefore, it is rotated relative to the B−P line so that it forms an angle B−H−H (denoted later β) with a maximal value of 111° (Figure 6g and Table 3). The structures of these TSs (Figure 6g,j) are similar to the one reported for the intramolecular trimethylene bridged FLP featuring $PMes_2$ and $B(C_6F_5)_2$ groups[52] and perfluoroboraada-mantane-based cryptands.[23]

Interestingly, there is an inverse relationship between H−P and H−H interatomic distances in TS2 (Figure 7) but not with
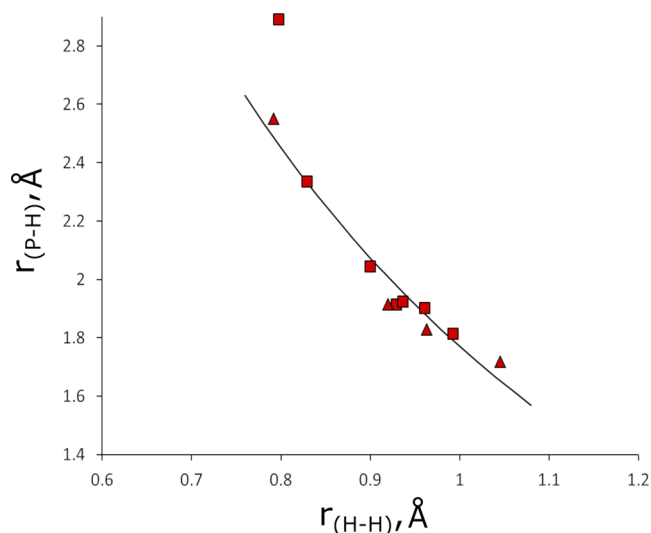

Figure 7. H−P vs H−H interatomic distances in optimized geometries of transition states LA···H···H···LB for all considered systems. Squares, B-containing systems; triangles, Al-containing systems. M06-2X/def2-TZVP level of theory.

B−H or Al−H distances (values in Å): $r(H-H) = (-0.97 \pm 0.26) + (2.73 \pm 0.24)/r(P-H)$ with $R^2 = 0.997$ if all TS2 are included in the fitting except for the one for the $B(C_6F_4)_3CF/PCy_3$ system. The latter TS is different from the others and is characterized by a short H−H bond, like in a hydrogen molecule, and a large interatomic distance between the nearest hydrogen and a phosphorus atom.

The noticeable polarization of the H_2 molecule in TS2 occurs when it is located between $B(C_6H_4)_3CH$ and P^tBu_3 (NPA charges for H$^-$ and H$^+$ are −0.034 and +0.23e). In all other considered pairs with B-containing Lewis acids, the NPA charges are positive for both hydrogen atoms of H_2, reflecting the fact that charge is transferred from the hydrogen molecule to the Lewis acid. Structurally, the TS2 leading to H_2 activation by complexes with $B(C_6F_4)_3CF$ is close to the $B(C_6F_4)_3CF·H_2$ intermediate. Relative to this intermediate state, the activation barriers are only 4 and 7 kJ·mol^{-1} for P^tBu_3 and PPh_3, respectively.

The $B(C_6F_4)_3CF/PCy_3$ is the only boron-containing system for which the LA·H_2 + LB intermediate was not located. The only TS located for this system features a rather short H−H bond (0.797 Å) and corresponds to the twisting of the H_2 molecule in the vicinity of the boron atom. No polarization of the H_2 molecule is observed in this TS, and both hydrogen atoms have similar NPA charges (+0.269 and +0.272). Any deviation from the TS geometry leads to hydrogen splitting forming the $[HPCy_3]^+[HB(C_6F_4)_3CF]^-$ ion pair, which is the most exergonic with respect to starting LA, LB, and H_2 among all considered systems (Table 2 and Figure 5).

The orbital interaction in the TS can be estimated via the difference of HOMO in the LB and LUMO of the LA·H_2 fragment. For complexes with $B(C_6F_5)_3$ derivatives, it was noted that the stronger LB has a lower HOMO[LB]−LUMO[LA·H_2] gap.[36] Indeed, for the 9-boratriptycene complexes, the smallest gap of 5.32 eV is observed for P^tBu_3 (see Table S1). However, for fluorinated LA, this gap is larger for PPh_3 than for P^tBu_3 due to the notable destabilizing of the LUMO energy level in [LA·H_2] of the fluorinated LA compared with 9-boratriptycene. Among the considered B-containing TS structures, the HOMO-[LB]−LUMO[LA·H_2] difference is minimal for B-$(C_6Me_4)_3CH/P^tBu_3$ (4.41 eV) and maximal for the B-$(C_6F_4)_3CF/PCy_3$ (5.87 eV) pairs.

We also considered the alternative reaction of the hydrogenation in the isolated LA with B−C bond cleavage (Figure 5,
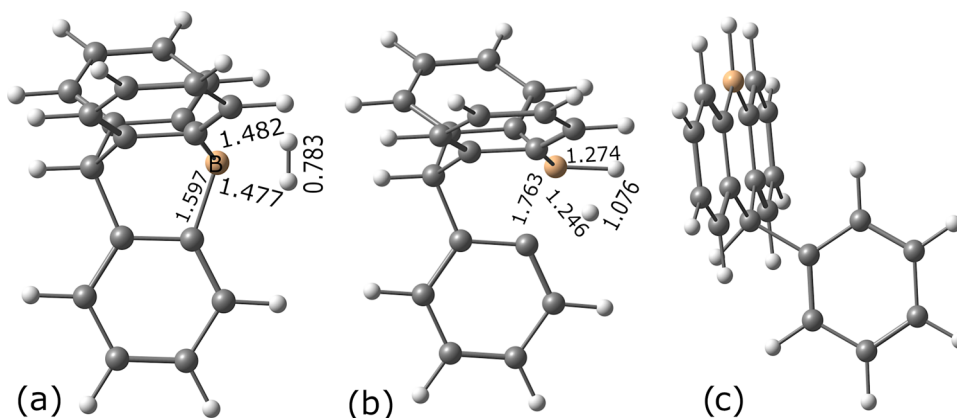

Figure 8. Optimized geometries for the $H_2·LA$ complex (a), TS (b), and reaction product **I** (c) for the hydrogenation of the C−B bond in $B(C_6H_4)_3CH$ without LB.

Table 4. Gas-Phase Relative Energies ΔE and Relative Standard Gibbs Energies $\Delta G°_{298}$ (kJ·mol^{-1}) of the Local Minima and Transition States for the Pathway of Hydrogenation of the C−B(Al) Bond without LB[a]

	ΔE	$\Delta G°_{298}$	ΔE	$\Delta G°_{298}$	ΔE	$\Delta G°_{298}$
LA	H$_2$·LA	H$_2$·LA	TS$_{LA}$	TS$_{LA}$	I	I
B(C$_6$Me$_4$)$_3$CH	−0.2	40.7	41.5	89.5	−141.5	−77.4
B(C$_6$H$_4$)$_3$CH	−28.8	11.9	19.4	64.7	−181.8	−136.9
B(C$_6$F$_4$)$_3$CF	−64.6	−21.2	7.5	53.8	−195.8	−146.6
Al(C$_6$H$_4$)$_3$CH	−20.9	11.3	64.4	102.5	−138.5	−99.6
Al(C$_6$F$_4$)$_3$CF	−42.8	−7.7	72.8	109.9	−148.1	−103.6

[a]The energies are given with respect to the sum of the energies of isolated components LA + H$_2$.

left side). Molecular hydrogen activation with B−C bond breaking was computationally studied for other compounds such as boroles[53,54] and the borinium cation [Mes$_2$B]$^+$.[55]

Optimized structures of the complex H$_2$·B(C$_6$H$_4$)$_3$CH, the transition state, and the reaction product **I** are presented in Figure 8. The overall process of B−C bond hydrogenation is highly exothermic and exergonic for all considered LA (Table 4).

It should be noted that the H$_2$·LA complexes (Figure 8a) are less energetically stable in the absence of LB. However, in terms of Gibbs energy, formation of H$_2$·B(C$_6$F$_4$)$_3$CF is more exergonic (−21.2 kJ mol^{-1}) than H$_2$·B(C$_6$F$_4$)$_3$CF···P^{t}Bu$_3$ (−9.7 kJ mol^{-1}) (Figure 6i) or H$_2$·B(C$_6$F$_4$)$_3$CF···PPh$_3$ (−19.5 kJ mol^{-1}). The transition states for B−C hydrogenation are notably higher in energy than the energies of the TS, leading to heterolytic H$_2$ splitting. However, Gibbs energy of TS$_{LA}$ for B(C$_6$Me$_4$)$_3$CH (89.5 kJ mol^{-1}) is lower than TS2 in B(C$_6$Me$_4$)$_3$CH/P^{t}Bu$_3$ (114.7 kJ mol^{-1}). In the case of B(C$_6$H$_4$)$_3$CH, the TS$_{LA}$ is higher in energy than TS2 in the B(C$_6$H$_4$)$_3$CH/P^{t}Bu$_3$ system (64.7 kJ mol^{-1} vs 48.3 kJ mol^{-1}). Thus, we conclude that the hydrogenation of B−C bonds is kinetically less favorable for B(C$_6$H$_4$)$_3$CH and B(C$_6$F$_4$)$_3$CF than heterolytic hydrogen splitting.

In the case of Al-containing Lewis acids, due to the formation of the strong DA complexes, the heterolytic hydrogen splitting is thermodynamically unfavorable and requires overcoming large energy barriers (109−139 kJ mol^{-1}), associated with splitting of the DA bond (Figure 9). Since for the methylated boron compound B(C$_6$Me$_4$)$_3$CH/P^{t}Bu$_3$ the hydrogen splitting was predicted to be endergonic and taking into account that on going from boron to aluminum the process will be even more endergonic,[23] we did not consider methylated aluminum derivatives.

The intermediate state in which a hydrogen molecule is captured by an aluminum atom was found only for the Al(C$_6$F$_4$)$_3$CF/P^{t}Bu$_3$ pair, but the geometry and the energy of this intermediate are close to the transition state TS2 for heterolytic hydrogen splitting. For other systems, the aluminum atom of LA is unable to "capture" the hydrogen molecule and the hydrogen splitting process is a one-step reaction leading from the DA complexes to the [HLB]$^+$[HLA]$^-$ ion pairs. The activation energies are 139, 121, 109, and 118 kJ·mol^{-1} for Al(C$_6$H$_4$)$_3$CH/P^{t}Bu$_3$, Al(C$_6$H$_4$)$_3$CH/PPh$_3$, Al(C$_6$F$_4$)$_3$CF/P^{t}Bu$_3$, and Al(C$_6$F$_4$)$_3$CF/PPh$_3$ pairs, respectively.

TS$_{LA}$ leading to hydrogenation of the Al−C bond without an LB is significantly higher in energy than the TS2 for both Al(C$_6$H$_4$)$_3$CH and Al(C$_6$F$_4$)$_3$CF (Figure 9), making heterolytic hydrogen splitting kinetically favorable.

Solvent Effect. It should be taken into account that the reaction of H$_2$ activation by FLP is strongly affected by the environment.[34] Solvent influence for FLP chemistry was
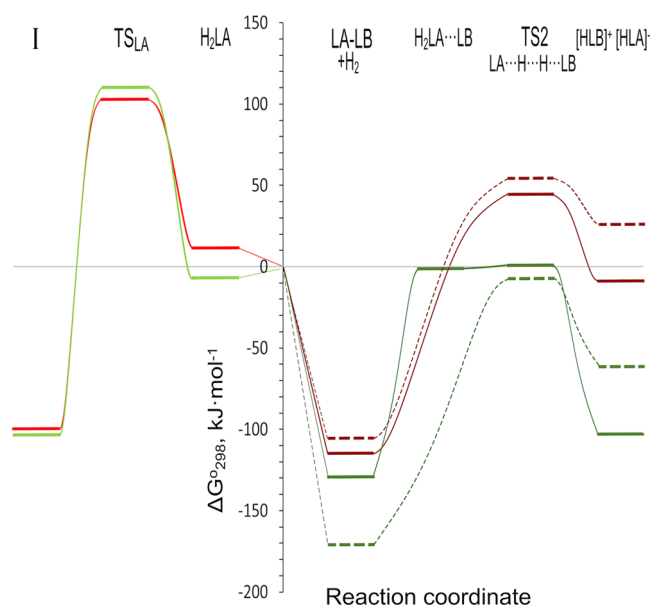

Figure 9. Reaction pathways for the hydrogenation of the Al−C bond without LB (left side) and heterolytic H$_2$ splitting (right side) for the aluminum-containing LA. Color code: Al(C$_6$H$_4$)$_3$CH (red) and Al(C$_6$F$_4$)$_3$CF (green); Lewis bases P^{t}Bu$_3$ (lines) and PPh$_3$ (dashed lines). The standard Gibbs energy values are given relative to the sum of the standard Gibbs energies of free components, LA + LB + H$_2$. M06-2X/def2-TZVP level of theory.

theoretically investigated by explicit[56] as well as implicit[57,58] solvation methods. A highly polar ion pair is stabilized in solution depending on the polarity of the solvent. The solvent contributions to the Gibbs energy of the reaction of H$_2$ activation by different intermolecular boron-phosphorus FLPs are from −4 to −32 kJ·mol^{-1} in toluene[58] and ca. −42 kJ·mol^{-1} in dichloromethane.[57]

To estimate the solvent effect on thermodynamic characteristics for the B(C$_6$H$_4$)$_3$CH/P^{t}Bu$_3$ system, single-point energy computations on gas-phase optimized geometries were carried out. SMD computations in the solvents for stationary states on the PES along the reaction path result in solvation free energy −39.8 kJ·mol^{-1} for the ion pair [HP^{t}Bu$_3$]$^+$ [HB(C$_6$H$_4$)$_3$CH]$^-$ in dichloromethane. Of these, −30.7 kJ·mol^{-1} accounts for electrostatic interactions with the solvent and −9.1 kJ·mol^{-1} for all nonelectrostatic interactions. The energies of stationary points (minima and TS) in solvents relative to free components are given in Table 5. Structural changes due to geometry optimization in the solvent are very minor. For example, in the B(C$_6$H$_4$)$_3$CH·P^{t}Bu$_3$ complexes, the B−P bond length decreases from 2.176 in the gas phase to 2.173 Å in toluene. The most notable change is the increase of the intermolecular distances in

Table 5. Relative Electronic Energies ΔE (with Respect to the Isolated LA, LB, and H$_2$, kJ·mol^{-1}) of Stationary Points along the Reaction Pathway for the Heterolytic H$_2$ Splitting by the B(C$_6$H$_4$)$_3$CH/P^{t}Bu$_3$ Lewis Pair in the Gas Phase and in the Solvents^a

stationary point	gas phase (opt)	toluene (opt)	toluene (SP)	dichloromethane (SP)
B(C$_6$H$_4$)$_3$CH·P^{t}Bu$_3$	−74.1	−69.3	−69.4	−73.6
(TS1) B(C$_6$H$_4$)$_3$CH···P^{t}Bu$_3$···H$_2$	−29.1	−24.9	−20.8	−17.6
H$_2$·B(C$_6$H$_4$)$_3$CH + P^{t}Bu$_3$	−65.8	−63.9	−62.6	−65.0
(TS2) B(C$_6$H$_4$)$_3$CH···H···H···P^{t}Bu$_3$	−46.4	−50.5	−50.3	−56.8
[HP^{t}Bu$_3$]$^+$[HB(C$_6$H$_4$)$_3$CH]$^-$	−106.4	−145.7	−143.1	−173.6

^{a}M06-2X/def2-TZVP level of theory.

the [HP^{t}Bu$_3$]$^+$[HB(C$_6$H$_4$)$_3$CH]$^-$ ionic pair. The H···H distance changes from 1.944 to 2.142 Å. However, even in this case, the overall energy difference is less than 3 kJ·mol^{-1} (Table 5).

Data obtained indicate that the solvent mainly stabilizes the final ion pair. It makes the overall reaction for the heterolytic hydrogen splitting more exothermic by 67.2 kJ·mol^{-1} in dichloromethane and by 36.7 kJ·mol^{-1} in toluene than in the gas phase. At the same time, the solvent has a small effect on the relative energies of the intermediates and transition states. Thus, the activation energies for the reaction in the gas phase satisfactory reproduce values in the solvents. Significant additional energetic stabilization of the final ionic pair [HP^{t}Bu$_3$]$^+$[HB(C$_6$H$_4$)$_3$CH]$^-$ in solution is similar to the values for other hydrogen splitting products reported in the literature.[57,58]

Comparison of the Studied Systems. Table 6 summarizes the most important characteristics of the studied systems

Table 6. Highest Activation Energy and Activation Gibbs Energy and Reaction Energies and Gibbs Energies for Heterolytic Hydrogen Splitting (in kJ mol^{-1}, Gas-Phase Values with Respect to the LA·LB Complex and H$_2$)^a

system	$\Delta E^{\#}$	$\Delta G^{\circ}_{298}{}^{\#}$	$\Delta_{(2)}E$	$\Delta_{(2)}G^{\circ}_{298}$
B(C$_6$Me$_4$)$_3$CH/P^{t}Bu$_3$	38.1	87.0	−28.5	27.6
B(C$_6$H$_4$)$_3$CH/P^{t}Bu$_3$	45.0	50.2	−32.4	−10.2
B(C$_6$H$_4$)$_3$CH/PCy$_3$	154.5	164.4	48.4	79.8
B(C$_6$H$_4$)$_3$CH/PPh$_3$	143.7	171.5	88.4	131.4
B(C$_6$F$_4$)$_3$CF/P^{t}Bu$_3$	−39.8	−28.1	−184.5	−167.2
B(C$_6$F$_4$)$_3$CF/PPh$_3$	114.1	144.0	14.7	51.0
B(C$_6$F$_4$)$_3$CF/PCy$_3$	162.9	176.5	−20.4	18.7
Al(C$_6$H$_4$)$_3$CH/P^{t}Bu$_3$	138.7	158.9	77.5	105.7
Al(C$_6$H$_4$)$_3$CH/PPh$_3$	120.6	159.3	78.9	131.2
Al(C$_6$F$_4$)$_3$CF/P^{t}Bu$_3$	109.1	130.0	−3.2	26.1
Al(C$_6$F$_4$)$_3$CF/PPh$_3$	117.8	163.7	63.3	109.1

^{a}M06-2X/def2-TZVP level of theory.

with respect to potential catalytic activity: the activation barriers and the reaction energies of heterolytic hydrogen splitting. The B(C$_6$Me$_4$)$_3$CH/P^{t}Bu$_3$ FLP system has a relatively large Gibbs activation energy of 87 kJ mol^{-1}, and the H$_2$ splitting is endergonic in the gas phase but the products are expected to be stabilized in solution. In contrast, the B(C$_6$F$_4$)$_3$CF/P^{t}Bu$_3$ FLP system exhibits barrierless highly exergonic splitting. In systems based on PCy$_3$ and PPh$_3$ Lewis bases, stable DA complexes are formed, which are ineffective for H$_2$ splitting.

Replacing a boron atom in 9-boratriptycene with an aluminum atom leads to an increase in LA pyramidalization and, consequently, to a decrease of steric repulsion. Strong DA bonds are formed with all phosphines, including P^{t}Bu$_3$. These complexes are predicted to split H$_2$ endergonically with large barriers and therefore are not suitable for practical applications.

Note however that artificially constrained donor−acceptor cryptands, featuring spatially separated Al and N centers preventing DA bond formation, are predicted to be highly active toward molecular hydrogen.[23,24]

Among the considered compounds, the most promising system for the creation of the catalytic cycle is the DA complex B(C$_6$H$_4$)$_3$CH·P^{t}Bu$_3$, which can be described as "latent" FLP. Despite the high B−P bond energy of 225 kJ mol^{-1}, the dissociation is facilitated by steric repulsion, and the enthalpy of dissociation of the complex is only 56 kJ mol^{-1}, which is below the "tipping point" of 60−100 kJ mol^{-1} for the dissociation equilibrium.[59] The overall process of heterolytic molecular hydrogen splitting is exergonic by 10 kJ mol^{-1} in the gas phase. The activation energy is only 45−56 kJ mol^{-1}, weakly depending on the medium.

The involvement of DA complexes in FLP reactivity was reported before. However, DA complexes were mostly considered handy examples for expanding the scope of FLP reactivity and not as primary synthetic targets. B(C$_6$F$_5$)$_3$ forms with lutidine a classical DA complex at low (−10 °C) temperatures, with a slightly elongated (by 0.033(4) Å) B−N distance compared to the complex with less basic pyridine. At room temperature, the complex undergoes equilibrium dissociation and heterolytically splits molecular hydrogen.[60] However, the process of hydrogen activation is not entirely reversible, since the resulting product [2,6-Me$_2$C$_5$H$_3$NH][HB-(C$_6$F$_5$)$_3$] completely loses H$_2$ only after addition of LB pyridine and heating to 100 °C for 8 h.[61] Irreversible H$_2$ activation was observed by covalently bonded monomeric phosphinoboranes R$_2$PB(C$_6$F$_5$)$_3$ (R = Cy, ^{t}Bu).[62] Formation of the "invisible" intramolecular FLP between camphor-bases enamine and HB(C$_6$F$_5$)$_2$ was deducted from the analysis of the hydrogen splitting products.[61]

Data obtained in the present work are in contrast to the statement that for reversible hydrogenation "the distance between LA and LB should be larger than 3 Å at least".[50] The latent FLP B(C$_6$H$_4$)$_3$CH·P^{t}Bu$_3$ has a much shorter B−P distance of 2.176 Å, but nevertheless it is a promising system for H$_2$ activation. Thus, it corroborates the statement of Fontaine and Stephan that "FLPs are defined by their reactivity rather than by their structural features".[63] Based on the experimental observation that the stable (undissociated) DA complex B(C$_6$F$_5$)$_3$·P(MeNCH$_2$CH$_2$)$_3$N forms FLP-type addition reactions with PhNCO, PhCH$_2$N$_3$, PhNSO, and CO$_2$, Stephan et al. point out the importance of exploring the reactivity of seemingly stable DA complexes.[64]

■ CONCLUSIONS

Geometries of the initial complexes between B(C$_6$R$_4$)$_3$CR (R = H, F, CH$_3$) and Al(C$_6$R$_4$)$_3$CR (R = H, F) with P^{t}Bu$_3$, PPh$_3$, and PCy$_3$, as well as reaction intermediates, transition states, and reaction products for heterolytic hydrogen splitting were

optimized at the M06-2X/def2-TZVP level of theory. Obtained results indicate that a combination of electronic and steric factors plays an important role in the DA complex or FLP formation in the reaction between 9-boratriptycene and its analogues with bulky phosphines. 9-Boratriptcene and its derivatives predominantly form DA complexes with phosphines. Only in the cases of $B(C_6Me_4)_3CH/P^tBu_3$ and $B(C_6F_4)_3CF/P^tBu_3$ systems frustrated Lewis pairs were observed (in the latter case, the DA complex is also formed). However, due to the different Lewis acidities, these FLPs exhibit quite different reactivities in hydrogen activation. The methyl-substituted derivative is predicted to split hydrogen endergonically (Gibbs energy change 28 kJ mol^{-1}) with the activation Gibbs energy of 87 kJ mol^{-1}. In contrast, for the F-substituted derivative, heterolytic hydrogen splitting is highly exergonic (by 167 kJ mol^{-1}) and is barrier-free. Resulting ion pairs are significantly stabilized in solution with respect to the gas phase, while the influence of the solvent on the energies of reaction intermediates and transition states is small.

The reaction of the H_2 molecule with considered pyramidal Lewis acids without a Lewis base results in hydrogenation with the splitting of B–C and Al–C bonds. This process is exothermic and exergonic for all studied LAs but is less kinetically favorable since it has larger activation energies than the process of heterolytic hydrogen splitting in the presence of LB.

Thus, we demonstrate that by varying the substituents on 9-boratriptycene and the bulkiness of the phosphine, a wide range of systems can be formed: from the strongly bound DA complexes, which are inactive in hydrogen splitting, to the FLP, which a highly exergonically split molecular hydrogen without a barrier. This opens the perspective of fine-tuning the Lewis acidity of 9-boratriptycene for the creation of FLP with the desired catalytic activity by changing the substituents.

It appears that there is an "optimal" degree of frustration required for reversibility in FLP chemistry. Too strong DA interactions favor the formation of strong DA bonds, which results in high activation barriers and thermodynamic unfavorability of hydrogen splitting. On the other hand, sterically overprotected FLPs have donor and acceptor centers located too far from each other. This decreases the internal electric field, which, together with orbital interactions,[65] is very important for heterolytic H_2 splitting[66] and increases the activation barriers. For very strong LA, the process of H_2 splitting is often too exergonic, which prevents reversibility.

Although the number of considered systems studied in the present work is rather small to make a definitive conclusion, it appears that "not so frustrated" or "latent" FLPs, which have a trade-off between the strong DA interaction energy and a steric repulsion, which still allows the components to form a complex with an elongated DA bond, are the best candidates for the construction of the equilibrium hydrogen splitting systems. We propose that by varying the substituents on 9-boratriptycene, it will be possible to construct systems that reversibly heterolytically split hydrogen with small energy barriers. We hope that our findings will stimulate future experimental and computational studies in this exciting area of chemistry, which is expected to be fruitful.

ASSOCIATED CONTENT

Supporting Information

The Supporting Information is available free of charge at https://pubs.acs.org/doi/10.1021/acsomega.2c06836.

Total energies, standard enthalpies, standard entropies, and optimized geometries (*xyz* coordinates) for all studied compounds and transition states, reaction energy diagrams, and selected characteristics of the considered transition states (PDF)

AUTHOR INFORMATION

Corresponding Author

Alexey Y. Timoshkin — *Institute of Chemistry, Saint Petersburg State University, 199034 St. Petersburg, Russia;* orcid.org/0000-0002-1932-6647; Email: a.y.timoshkin@spbu.ru

Author

Anna V. Pomogaeva — *Institute of Chemistry, Saint Petersburg State University, 199034 St. Petersburg, Russia;* orcid.org/0000-0002-5131-4240

Complete contact information is available at:
https://pubs.acs.org/10.1021/acsomega.2c06836

Notes

The authors declare no competing financial interest.

REFERENCES

(1) Welch, G. C.; San Juan, R. R.; Masuda, J. D.; Stephan, D. W. Reversible, Metal-Free Hydrogen Activation. *Science* **2006**, *314*, 1124–1126.

(2) Stephan, D. W.Discovery of Frustrated Lewis Pairs: Intermolecular FLPs for Activation of Small Molecules. In *Topics in Current Chemistry*; Erker, G.; Stephan, D., Eds.; Springer: Berlin, 2013; Vol. 332, pp 1–44.

(3) Chen, D.; Klankermayer, J.Frustrated Lewis Pairs: From Dihydrogen Activation to Asymmetric Catalysis. In *Topics in Current Chemistry*; Erker, G.; Stephan, D., Eds.; Springer: Berlin, 2013; Vol. 334, pp 1–26.

(4) Stephan, D. W. Frustrated Lewis Pairs. *J. Am. Chem. Soc.* **2015**, *137*, 10018–10032.

(5) Khan, I.; Manzotti, M.; Tizzard, G. J.; Coles, S. J.; Melen, R. L.; Morrill, L. C. Frustrated Lewis Pair (FLP)-Catalyzed Hydrogenation of Aza-Morita–Baylis–Hillman Adducts and Sequential Organo-FLP Catalysis. *ACS Catal.* **2017**, *7*, 7748–7752.

(6) Melen, R. L. A Step Closer to Metal-Free Dinitrogen Activation: A New Chapter in the Chemistry of Frustrated Lewis Pairs. *Angew. Chem., Int. Ed.* **2018**, *57*, 880–882.

(7) Stephan, D. W.; Erker, G. Frustrated Lewis Pair Chemistry: Development and Perspectives. *Angew. Chem., Int. Ed.* **2015**, *54*, 6400–6441.

(8) Stephan, D. W. Diverse Uses of the Reaction of Frustrated Lewis Pair (FLP) with Hydrogen. *J. Am. Chem. Soc.,* **2021**, *143*, 20002–20014.

(9) (a) Harman, W. H.; Peters, J. C. Reversible H_2 Addition across a Nickel–Borane Unit as a Promising Strategy for Catalysis. *J. Am. Chem. Soc.* **2012**, *134*, 5080–5082. (b) Su, Y.; Li, Y.; Ganguly, R.; Kinjo, R. Engineering the Frontier Orbitals of a Diazadiborinine for Facile Activation of H_2, NH_3, and an Isonitrile. *Angew. Chem., Int. Ed.* **2018**, *57*, 7846–7849. (c) Prey, S. E.; Wagner, M. Threat to the Throne: Can Two Cooperating Boron Atoms Rival Transition Metals in Chemical Bond Activation and Catalysis? *Adv. Synth. Catal.* **2021**, *363*, 2290–2309. (d) Schultz, J.; Sárosi, M. B.; Hey-Hawkins, E. Exploring the Reactivity of B-Connected Carboranylphosphines in Frustrated Lewis Pair Chemistry: A New Frame for a Classic System. *Chem. — Eur. J.* **2022**, *28*, No. e202200531.

(10) Nicasio, J. A.; Steinberg, S.; Inés, B.; Alcarazo, M. Tuning the Lewis Acidity of Boranes in Frustrated Lewis Pair Chemistry: Implications for the Hydrogenation of Electron-Poor Alkenes. *Chem. − Eur. J.* **2013**, *19*, 11016−11020.

(11) Yin, Q.; Kemper, S.; Klare, H. F. T.; Oestreich, M. Boron Lewis Acid-Catalyzed Hydroboration of Alkenes with Pinacolborane: BAr$_3^{\text{F}}$ Does What B(C$_6$F$_5$)$_3$ Cannot Do! *Chem. − Eur. J.* **2016**, *22*, 13840−13844.

(12) Kögel, J. F.; Timoshkin, A. Y.; Schröder, A.; Lork, E.; Beckmann, J. Al(OCAr$_3^{\text{F}}$)$_3$ − a thermally stable Lewis superacid. *Chem. Sci.* **2018**, *9*, 8178−8183.

(13) Stoian, C.; Olaru, M.; Cucuieţ, T. A.; Kegyes, K. T.; Sava, A.; Timoshkin, A. Y.; Raţ, C. I.; Beckmann, J. Bulky Polyfluorinated Terphenyldiphenylboranes: Water Tolerant Lewis Acids. *Chem. − Eur. J.* **2021**, *27*, 4327−4331.

(14) Timoshkin, A. Y.; Frenking, G. Gas-Phase Lewis Acidity of Perfluoroaryl Derivatives of Group 13 Elements. *Organometallics* **2008**, *27*, 371−380.

(15) Davydova, E. I.; Sevastianova, T. N.; Timoshkin, A. Y. Molecular complexes of group 13 element trihalides, pentafluorophenyl derivatives and Lewis superacids. *Coord. Chem. Rev.,* **2015**, *297-298*, 91−126.

(16) Mück, L. A.; Timoshkin, A. Y.; von Hoppfgarten, M.; Frenking, G. Donor Acceptor Complexes of Noble Gases. *J. Am. Chem. Soc.* **2009**, *131*, 3942−3949.

(17) Mück, L. A.; Timoshkin, A. Y.; Frenking, G. Design of Neutral Lewis Superacids of Group 13 Elements. *Inorg. Chem.* **2012**, *51*, 640−646.

(18) Gilbert, T. M. Computational studies of complexation of nitrous oxide by borane−phosphine frustrated Lewis pairs. *Dalton Trans.* **2012**, *41*, 9046−9055.

(19) Chardon, A.; Osi, A.; Mahaut, D.; Ben Saida, A.; Berionni, G. Non-planar Boron Lewis Acids Taking the Next Step: Development of Tunable Lewis Acids, Lewis Superacids and Bifunctional Catalysts. *Synlett* **2020**, *31*, 1639−1648.

(20) Wood, T. K.; Piers, W. E.; Keay, B. A.; Parvez, M. 1-Borabarrelene Derivatives via Diels−Alder Additions to Borabenzenes. *Org. Lett.* **2006**, *8*, 2875−2878.

(21) Mikhailov, B. M. The chemistry of boron-cage compounds. *Pure Appl. Chem.* **1980**, *52*, 691−704.

(22) Bubnov, Y. N.; Gurskii, M. E.; Pershin, D. G.; Lyssenko, K. A.; Antipin, M. Y. Complexes of 1-boraadamantane and its derivatives with 1-azaadamantanes: Synthesis and molecular structure. *Russ. Chem. Bull.* **1998**, *47*, 1771−1777.

(23) El-Hamdi, M.; Timoshkin, A. Y. Hydrogen splitting by pyramidalized 13−15 donor−acceptor cryptands: A computational study. *J. Comput. Chem.* **2019**, *40*, 1892−1901.

(24) Timoshkin, A. Y.; Morokuma, K. Novel group 13 Lewis superacids and 13−15 donor−acceptor cryptands for hydrogen activation: a theoretical study. *Phys. Chem. Chem. Phys.* **2012**, *14*, 14911−14916.

(25) Ben Saida, A.; Chardon, A.; Osi, A.; Tumanov, N.; Wouters, J.; Adjieufack, A. I.; Champagne, B.; Berionni, G. Pushing the Lewis Acidity Boundaries of Boron Compounds With Non-Planar Triarylboranes Derived from Triptycenes. *Angew. Chem., Int. Ed.* **2019**, *58*, 16889−16893.

(26) Chardon, A.; Osi, A.; Mahaut, D.; Doan, T.-H.; Tumanov, N.; Wouters, J.; Fusaro, L.; Champagne, B.; Berionni, G. Controlled Generation of 9-Boratriptycene by Lewis Adduct Dissociation: Accessing a Non-Planar Triarylborane. *Angew. Chem., Int. Ed.* **2020**, *59*, 12402−12406.

(27) Henkelmann, M.; Olmor, A.; Bolte, M.; Schünemann, V.; Lerner, H.-W.; Noga, J.; Hrobárik, P.; Wagner, M. A free boratriptycene-type Lewis superacid. *Chem. Sci.* **2022**, *13*, 1608−1617.

(28) Osi, A.; Mahaut, D.; Tumanov, N.; Fusaro, L.; Wouters, J.; Champagne, B.; Chardon, A.; Berionni, G. Taming the Lewis Superacidity of Non-Planar Boranes: C−H Bond Activation and Non-Classical Binding Modes at Boron. *Angew. Chem., Int. Ed.* **2022**, *61*, No. e202112342.

(29) Mahaut, D.; Chardon, A.; Mineur, L.; Berionni, G.; Champagne, B. Rational Development of a Metal-Free Bifunctional System for the C-H Activation of Methane: A Density Functional Theory Investigation. *ChemPhysChem* **2021**, *22*, 1958−1966.

(30) Mayer, U.; Gutmann, V.; Gerger, W. The acceptor number - A quantitative empirical parameter for the electrophilic properties of solvents. *Monatsh. Chem.* **1975**, *106*, 1235−1257.

(31) Sivaev, I. B.; Bregadze, V. I. Lewis acidity of boron compounds. *Coord. Chem. Rev.* **2014**, *270−271*, 75−88.

(32) Pu, M.; Privalov, T. How Frustrated Lewis Acid/Base Systems Pass through Transition-State Regions: H$_2$ Cleavage by [tBu$_3$P/B(C$_6$F$_5$)$_3$]. *ChemPhysChem* **2014**, *15*, 2936−2944.

(33) Liu, L.; Lukose, B.; Ensing, B. Hydrogen Activation by Frustrated Lewis Pairs Revisited by Metadynamics Simulations. *J. Phys. Chem. C* **2017**, *121*, 2046−2051.

(34) Liu, L.; Lukose, B.; Jaque, P.; Ensing, B. Reaction mechanism of hydrogen activation by frustrated Lewis pairs. *Green Energy Environ.* **2019**, *4*, 20−28.

(35) Wang, L.; Kehr, G.; Daniliuc, C. G.; Brinkkötter, M.; Wiegand, T.; Wübker, A.-L.; Eckert, H.; Liu, L.; Brandenburg, J. G.; Grimme, S.; Erker, G. Solid state frustrated Lewis pair chemistry. *Chem. Sci.* **2018**, *9*, 4859−4865.

(36) Heshmat, M.; Ensing, B. Optimizing the Energetics of FLP-Type H$_2$ Activation by Modulating the Electronic and Structural Properties of the Lewis Acids: A DFT Study. *J. Phys. Chem. A* **2020**, *124*, 6399−6410.

(37) Piers, W. E.; Marwitz, A. J. V.; Mercier, L. G. Mechanistic Aspects of Bond Activation with Perfluoroarylboranes. *Inorg. Chem.* **2011**, *50*, 12252−12262.

(38) Zhao, Y.; Truhlar, D. G. The M06 suite of density functionals for main group thermochemistry, thermochemical kinetics, noncovalent interactions, excited states, and transition elements: two new functionals and systematic testing of four M06-class functionals and 12 other functionals. *Theor. Chem. Acc.* **2008**, *120*, 215−241.

(39) Weigend, F.; Ahlrichs, R. Balanced basis sets of split valence, triple zeta valence and quadruple zeta valence quality for H to Rn: Design and assessment of accuracy. *Phys. Chem. Chem. Phys.* **2005**, *7*, 3297−3305.

(40) Frisch, M. J.; Trucks, G. W.; Schlegel, H. B.; Scuseria, G. E.; Robb, M. A.; Cheeseman, J. R.; Scalmani, G.; Barone, V.; Petersson, G. A.; Nakatsuji, H.; Li, X.; Caricato, M.; Marenich, A. V.; Bloino, J.; Janesko, B. G.; Gomperts, R.; Mennucci, B.; Hratchian, H. P.; Ortiz, J. V.; Izmaylov, A. F.; Sonnenberg, J. L.; Williams-Young, D.; Ding, F.; Lipparini, F.; Egidi, F.; Goings, J.; Peng, B.; Petrone, A.; Henderson, T.; Ranasinghe, D.; Zakrzewski, V. G.; Gao, J.; Rega, N.; Zheng, G.; Liang, W.; Hada, M.; Ehara, M.; Toyota, K.; Fukuda, R.; Hasegawa, J.; Ishida, M.; Nakajima, T.; Honda, Y.; Kitao, O.; Nakai, H.; Vreven, T.; Throssell, K.; Montgomery, J. A., Jr; Peralta, J. E.; Ogliaro, F.; Bearpark, M. J.; Heyd, J. J.; Brothers, E. N.; Kudin, K. N.; Staroverov, V. N.; Keith, T. A.; Kobayashi, R.; Normand, J.; Raghavachari, K.; Rendell, A. P.; Burant, J. C.; Iyengar, S. S.; Tomasi, J.; Cossi, M.; Millam, J. M.; Klene, M.; Adamo, C.; Cammi, R.; Ochterski, J. W.; Martin, R. L.; Morokuma, K.; Farkas, O.; Foresman, J. B.; Fox, D. J.*Gaussian 16*, revision B.01; Gaussian, Inc.: Wallingford, CT, 2016.

(41) Fukui, K. The path of chemical reactions - the IRC approach. *Acc. Chem. Res.* **1981**, *14*, 363−368.

(42) Page, M.; McIver, J. W., Jr. On evaluating the reaction path Hamiltonian. *J. Chem. Phys.* **1988**, *88*, 922−935.

(43) Marenich, A. V.; Cramer, C. J.; Truhlar, D. G. Universal Solvation Model Based on Solute Electron Density and on a Continuum Model of the Solvent Defined by the Bulk Dielectric Constant and Atomic Surface Tensions. *J. Phys. Chem. B* **2009**, *113*, 6378−6396.

(44) Timoshkin, A. Y.; Suvorov, A. V.; Bettinger, H. F.; Schaefer, H. F. Role of the Terminal Atoms in the Donor−Acceptor Complexes MX$_3$−D (M = Al, Ga, In; X = F, Cl, Br, I; D = YH$_3$, YX$_3$, X$^-$; Y = N, P, As). *J. Am. Chem. Soc.* **1999**, *121*, 5687−5699.

(45) Mantina, M.; Chamberlin, A. C.; Valero, R.; Cramer, C. J.; Truhlar, D. G. Consistent van der Waals Radii for the Whole Main Group. *J. Phys. Chem. A* **2009**, *113*, 5806−5812.

(46) Ketkov, S.; Rychagova, E.; Kather, R.; Beckmann, J. Pnictogen effects on the electronic interactions in the Lewis pair complexes $Ph_3EB(C_6F_5)_3$ (E = P, As, Sb). *J. Organomet. Chem.* **2021**, *949*, No. 121944.

(47) Gusev, D. G. Donor Properties of a Series of Two-Electron Ligands. *Organometallics* **2009**, *28*, 763−770.

(48) Mo, L.; Barr, H. I.; Odom, A. L. Investigation of phosphine donor properties to vanadium(V) nitrides. *Results Chem.* **2022**, *4*, No. 100344.

(49) Kaehler, T.; Melen, R. L. Comparative study of fluorinated triarylalanes and their borane counterparts. *Cell Rep. Phys. Sci.* **2021**, *2*, No. 10100595.

(50) Wang, K.; Pan, Z.; Xu, W.; Chen, Z.; Yu, X. The preconditions of reversible hydrogenation−dehydrogenation of B/N and B/P frustrated Lewis Pairs. *J. Energy Chem.* **2019**, *35*, 174−180.

(51) Sumerin, V.; Schulz, F.; Nieger, M.; Atsumi, M.; Wang, C.; Leskelä, M.; Pyykkö, P.; Repo, T.; Rieger, B. Experimental and theoretical treatment of hydrogen splitting and storage in boron− nitrogen systems. *J. Organomet. Chem.* **2009**, *694*, 2654−2660.

(52) Özgün, T.; Bergander, K.; Liu, L.; Daniliuc, C. G.; Grimme, S.; Kehr, G.; Erker, G. A Frustrated Phosphane−Borane Lewis Pair and Hydrogen: A Kinetics Study. *Chem. − Eur. J.* **2016**, *22*, 11958−11961.

(53) Qu, Z.-W.; Zhu, H. Toward Reversible Dihydrogen Activation by Borole Compounds,. *J. Phys. Chem. C* **2013**, *117*, 11989−11993.

(54) Houghton, A. Y.; Karttunen, V. A.; Piers, W. E.; Tuononen, H. M. Hydrogen activation with perfluorinated organoboranes: 1,2,3-tris-(pentafluorophenyl)-4,5,6,7-tetrafluoro-1-boraindene. *Chem. Commun.* **2014**, *50*, 1295−1298.

(55) Bamford, K. L.; Qu, Z.-W.; Stephan, D. W. Activation of H_2 and Et_3SiH by the Borinium Cation $[Mes_2B]^+$: Avenues to Cations $[MesB(\mu\text{-}H)_2(\mu\text{-}Mes)BMes]^+$ and $[H_2B(\mu\text{-}H)(\mu\text{-}Mes)B(\mu\text{-}Mes)(\mu\text{-}H)BH_2]^+$. *J. Am. Chem. Soc.* **2019**, *141*, 6180−6184.

(56) Bakó, I.; Stirling, A.; Balint, S.; Papai, I. Association of frustrated phosphine−borane pairs in toluene: molecular dynamics simulations. *Dalton Trans.* **2012**, *41*, 9023−9025.

(57) Schirmer, B.; Grimme, S.Quantum Chemistry of FLPs and Their Activation of Small Molecules: Methodological Aspects. In *Topics in Current Chemistry*; Erker, G.; Stephan, D., Eds.; Springer, 2013; Vol. *332*, pp 213−230.

(58) Liu, X.; Li, X.; Yao, X.; Zhao, W.; Liu, L. Effects of Ionic Liquids on the Thermodynamics of Hydrogen Activation by Frustrated Lewis Pairs: A Density Functional Theory Study. *ChemPhysChem* **2021**, *22*, 968−974.

(59) Geier, S. J.; Gille, A. L.; Gilbert, T. M.; Stephan, D. W. From Classical Adducts to Frustrated Lewis Pairs: Steric Effects in the Interactions of Pyridines and $B(C_6F_5)_3$. *Inorg. Chem.* **2009**, *48*, 10466−10474.

(60) Geier, S. J.; Stephan, D. W. Lutidine/$B(C_6F_5)_3$: At the Boundary of Classical and Frustrated Lewis Pair Reactivity. *J. Am. Chem. Soc.* **2009**, *131*, 3476−3477.

(61) Schwendemann, S.; Oishi, S.; Saito, S.; Fröhlich, R.; Kehr, G.; Erker, G. Reaction of an "Invisible" Frustrated N/B Lewis Pair with Dihydrogen. *Chem. − Asian J.* **2013**, *8*, 212−217.

(62) Geier, S. J.; Gilbert, T. M.; Stephan, D. W. Activation of H_2 by Phosphinoboranes $R_2PB(C_6F_5)_2$. *J. Am. Chem. Soc.,* **2008**, *130*, 12632−12633.

(63) Fontaine, F.-G.; Stephan, D. W. On the concept of frustrated Lewis pairs. *Philos. Trans. R. Soc. A* **2017**, *375*, No. 20170004.

(64) Johnstone, T. C.; Wee, G. N. J. H.; Stephan, D. W. Accessing Frustrated Lewis Pair Chemistry from a Spectroscopically Stable and Classical Lewis Acid-Base Adduct. *Angew. Chem., Int. Ed.* **2018**, *57*, 5881−5884.

(65) Rokob, T. A.; Hamza, A.; Stirling, A.; Soós, T.; Pápai, I. Turning Frustration into Bond Activation: A Theoretical Mechanistic Study on Heterolytic Hydrogen Splitting by Frustrated Lewis Pairs. *Angew. Chem., Int. Ed.* **2008**, *47*, 2435−2438.

(66) Grimme, S.; Kruse, H.; Goerigk, L.; Erker, G. The Mechanism of Dihydrogen Activation by Frustrated Lewis Pairs Revisited. *Angew. Chem., Int. Ed.* **2010**, *49*, 1402−1405.